

Rutherford Scattering of α -Particles

Emily P. Wang*

MIT Department of Physics

(Dated: December 8, 2004)

The scattering of α -particles off of gold foil was investigated. Attenuation of the α -particle beam was used to measure the thickness of the gold foil used. The coefficient of the Rutherford differential scattering cross section was experimentally determined to be $(7.81 \pm 5.35) \times 10^{-25} \text{cm}^2$, compared to $1.76 \times 10^{-24} \text{cm}^2$, with a reduced chi-squared of 3.4, which is a reasonable fit and confirms the accuracy of the Rutherford model of the atom.

1. INTRODUCTION

When Geiger and Marsden first began scattering experiments involving alpha particles and thin metal foils, scientists knew little about the structure of the atom. The charge to mass ratio of the electron was known with reasonable accuracy, and it was also known that most of the mass in an atom was due to the positive charge. The dilemma faced by scientists was understanding how the positive and negative components of the atom were held together, and how they managed to create the regular phenomena that had been observed, such as the combination rules and series limits for the complex spectra of multi-electron atoms.

Drawing upon Newtonian mechanics and Maxwell's electromagnetic theory, J. J. Thompson formulated the "plum-pudding" model of the atom. In this model, the atom consisted of a spherical "pudding" of positive charge, and electrons were distributed throughout the atom, much like raisins in a pudding. The drawbacks of the plum-pudding model was that it yielded no explanation for the quantized nature of the hydrogen spectrum, as expressed by the Balmer formula and the Ritz combination principle for atomic spectra.

Rutherford came upon the idea of probing the structure of atom by firing α -particles, or helium ions, at thin metal foils. The experiments conducted by Rutherford and his collaborators Geiger and Marsden lead to a revolution in the model of atomic structure. If the plum-pudding model had indeed been correct, then the fraction of particles scattered through an angle of θ or greater should have been observed to fall off like a Gaussian. This description was found to be accurate for small angle scattering, but not for large angles of scattering [1].

The goal of this experiment was to reproduce Rutherford's experiment with thin metal foils by scattering alpha particles through a gold foil. Experimental data was compared to the theoretical model of Rutherford scattering.

2. DIFFERENTIAL SCATTERING CROSS SECTION OF NUCLEI

For a single scatterer, such as a single gold nucleus within a thin gold foil layer, the differential scattering cross section is defined as follows [2]:

$$\frac{d\sigma(\theta, \phi)}{d\Omega} = \frac{\text{flux scattered into element } d\Omega \text{ at angles } (\theta, \phi)}{\text{incident flux per unit area}}$$

where σ is the scattering cross section of a single nucleus. To obtain the differential scattering cross section, one can make measurements of the intensity I_θ of the beam when alpha particles are scattered through certain angles θ and calculate as follows:

$$\frac{d\sigma}{d\Omega} = \frac{I_\theta \times A}{d\Omega \times I_0 \times N_{Avo} \times \rho \times x_{foil}} \quad (1)$$

where N_{Avo} is Avogadro's number, x_{foil} is the thickness of the target foil, A is the atomic mass of the material in the target foil, $d\Omega$ is the solid-angle of the detector, I_0 is the unattenuated intensity of the alpha particle beam.

Using classical mechanics to calculate the effect on alpha particles as they approached atomic nuclei, Rutherford derived an equation to describe the scattering of particles at large angles, where scattering is mostly due to a single scattering event rather than multiple small angle scattering events. Laborious experiments conducted by Geiger and Marsden found this equation to hold true. The equation is as follows [3]:

$$\frac{d\sigma}{d\Omega} = \left(\frac{ZZ'e^2}{4E}\right)^2 \frac{1}{\sin^4\left(\frac{\theta}{2}\right)} \quad (2)$$

where Ze is the charge of the target nuclei, $Z'e$ is the charge of the alpha particles, and E is the kinetic energy of the alpha particles.

3. SOLID-STATE DETECTORS

Solid-state detectors hold several advantages over their gas-filled counterparts. One advantage is the greater resolution and better statistics possible, due to the fact that lower energy is needed for the creation of

*Electronic address: wangfire@mit.edu

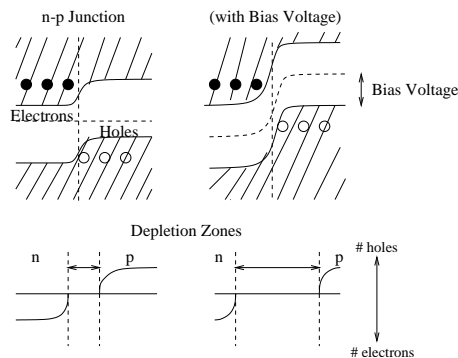


FIG. 1: The upper two images show an n-p semi-conductor junction before and after bias voltage is turned on. The lower two images show the depletion zone in each case—note that the depletion zone length is increased with the addition of bias voltage. Figure adapted from [4]

electron-ion pairs. Another advantage is the greater stopping power of the solid-state detector, which allows the detection of particles with energies characteristic of nuclear interactions [4]. As the alpha particle beam was to be interacting with the nuclei of atoms in this experiment, a silicon barrier detector, one type of solid-state detector, was used for counting purposes.

For the best results, semi-conductor junctions are used in most solid-state detectors—these detectors are also known as barrier layer detectors. An n-p semi-conductor junction is shown in Figure 1. On the left-hand side of the junction is the n-type semiconductor, which donates negative charge carriers, or electrons. On the right-hand side of the junction is the p-type semiconductor, which donates positive charge carriers, or holes. There is an area between the n- and p-type materials where there are neither positive nor negative charge carriers present, and this area is called the “depletion zone”. It is in this region of the detector that the electron-ion pairs are formed and detected. An alpha particle enters from the n side of the junction and forms an electron-ion pair in the depletion zone. Critical to the effectiveness of these barrier detectors is the bias voltage, which serves to increase the length of the depletion zone. The longer the depletion zone, the greater the fraction of alpha particles that will be captured and detected. For achieving good resolution in the solid-state detector, then, the length of the depletion zone must be sufficiently large. Once the electron-ion pair forms in the depletion zone, the two charges are accelerated in opposite directions, and this acceleration of charges causes a current that registers in the detector [4].

4. EXPERIMENTAL SETUP AND OBTAINING BEAM PROFILE

The setup for the experiment is shown in Figure 2. In conducting the experiment, the first step was to cover the

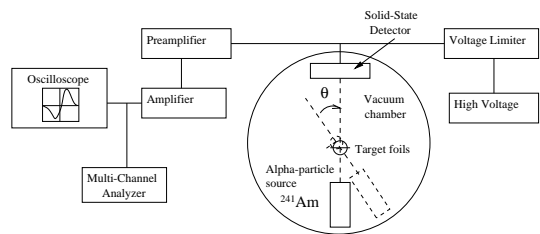


FIG. 2: Setup of equipment used for both open-aperture and attenuated beam measurements, as well as angular dependence of differential scattering cross section. The vacuum chamber was maintained at approximately 200 microns, or 10^{-3} torr

vacuum chamber with a clear plexiglass cover weighted down with lead bricks (in order to ensure the o-ring along the rim of the vacuum chamber achieved a good seal). With the bias voltage on the silicon barrier detector turned down, the air was then pumped out of the cylindrical vacuum chamber. After the pressure in the chamber was on the order of 200 microns, the lead bricks were removed from the plexiglass cover and a thick black cloth sheath was placed over the vacuum chamber. The bias voltage of the system was then slowly turned up to approximately +52V. To protect the detector, the cloth cover was placed over the vacuum chamber whenever the bias voltage was turned up—it was necessary to turn down the bias voltage whenever adjustments in the alpha particle beam source needed to be made.

The first part of this experiment involved calculating the thickness of the gold foil targets and characterizing the profile of the alpha particle beam. The target foils were mounted in a small, flat, rectangular piece of metal that contained several holes, some of which had metal foils secured over them, and some of which were left open for open-aperture measurements. The rectangular piece of metal containing the open aperture and the target foils was placed approximately 8 cm away from the point where the alpha particles emerged from the source. One experimental consideration was the height of the target foils and open aperture relative to the alpha particle beam height—to determine the optimal position, the countrate was recorded for different heights in 2mm increments, and the vertical positioning with the maximum number of counts was recorded and used in subsequent measurements.

To measure the beam profile, the height of the target foil holder was set for the open aperture, and the beam was allowed to impinge upon the detector at angles ranging from -6 degrees to 8 degrees with the normal. The total number of counts over run times ranging from 100 seconds (for smaller angles) to 300 seconds (for $\pm 6^\circ$ and 9°) was determined for each angular position. This was done by noting the MCS spectrum output and summing over all channels of the peak. The countrate was determined for each angle measurement and was plotted, as shown in Figure 3. The shape of the beam profile is approximately

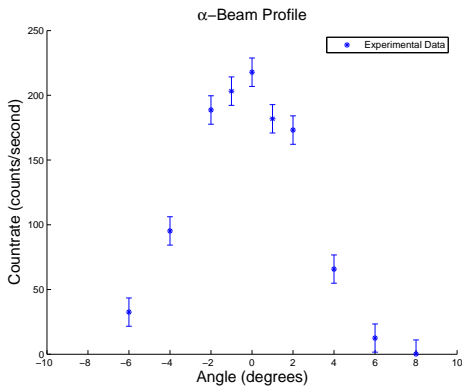


FIG. 3: Beam profile at open aperture. This represents a convolution of the the detector area with the area of the alpha beam emerging from the source.

triangular, with a base half-width of approximately 7 degrees. The explanation for this shape can be understood by recognizing the fact that the beam profile represents the convolution between the shape of the alpha particle beam emerging from the source and the shape of the detector. The alpha particle beam is highly collimated and can hence be considered to have an angular behavior that is roughly square. The detector is sensitive and detects any particle that impinges upon it, so its behavior can also be considered to be a square. The convolution of two square profiles will be triangular, and this is what we observe in the beam profile. The implications of having a finite alpha particle source are discussed in the Analysis section.

5. BEAM ATTENUATION

To determine the thickness of the foils, measurements of the beam intensity at zero degrees were taken and the decrease in energy of the α -particles was noted. The same setup was used and the target foil holder was set so that the α -particles impinged upon the target with four layers of gold foil. The channel number of the peak of the alpha particle beam in the MCS spectrum was noted—this channel number was directly proportional to the energy of the peak. The peak location was compared to that of the unattenuated beam, which was known to have an energy of 5.486 MeV. The following equation was used to obtain the energy of the attenuated beam:

$$E_2 = \frac{c_2}{c_1} E_1 \quad (3)$$

where c_1 was the channel number of the unattenuated beam's peak, c_2 was the channel number of the attenuated beam's peak, E_1 was the energy of the unattenuated beam, and E_2 was the energy of the attenuated beam. Measurements were also taken for the target that consisted of eight layers of gold foil.

TABLE I: Beam Attenuation Data

Target	Peak (MeV)	Range ^a ($10^{-3}g/cm^2$)	Thickness ($10^{-3}g/cm^2$)
None	5.486	18.04	N/A
Au (4 layers)	3.115	8.787	9.256 ± 0.711
Au (8 layers)	0.791	2.284	15.78 ± 0.439

^aProjected range of α -particles in Au was obtained from <http://physics.nist.gov/PhysRefData/Star/Text/ASTAR.html>.

TABLE II: Gold Foil (4 Layers) Scattering Data

Angle ($^{\circ}$)	Duration (sec)	I_0^a (cts/sec)	Total counts	Countrate (I) (10^{-3} cts/sec)
30 ± 0.4	600	245.9 ± 2.03	58 ± 7.6	97 ± 13
40 ± 0.4	3493	244.9 ± 2.02	74 ± 8.6	21 ± 2.5
45 ± 0.4	1347	245.9 ± 2.03	21 ± 4.6	16 ± 3.4
50 ± 0.4	60917	244.9 ± 2.02	502 ± 22.4	$8.2 \pm .37$
60 ± 0.4	5306	245.9 ± 2.03	13 ± 3.6	$2.5 \pm .68$

^aThis represents the intensity of the beam while passing through open aperture. There were small fluctuations in countrate from day to day, so the I_0 from each day was used to normalize all of the data.

By using online NIST data ([5]), the projected range of the α -particles was obtained for the energies measured for targets of 4 layers of gold foil and 8 layers of gold foil. These projected ranges were subtracted from the projected range of the 5.496 MeV α -particles in the unattenuated beam to obtain the thickness of the gold foils in g/cm^2 . Results are shown in Table I.

6. SCATTERING FROM GOLD FOILS

The next part of the experiment involved observing the angular dependence of alpha particles scattered through gold foil. Again, the setup shown above was used, and the target foil holder adjusted so that the alpha particle beam illuminated the four layers of gold foil. Measurements of average countrate were taken with the alpha beam positioned at angles from 30 to 60 degrees, with run times ranging from 600 seconds to about 60,000 seconds. The MCS Measurements taken at larger angles were taken with longer run times due to the lower counrates. The raw data is displayed in Table II.

Because the experiment was conducted over approximately two weeks, it was necessary to normalize data taken separate days to the I_0 measured on each respective day. This was done by taking a 60 second long, 0° measurement of the alpha particle beam seen through the open aperture on each day. Counrates obtained on that day were divided by the open aperture countrate to produce a relative countrate of $\frac{I}{I_0}$.

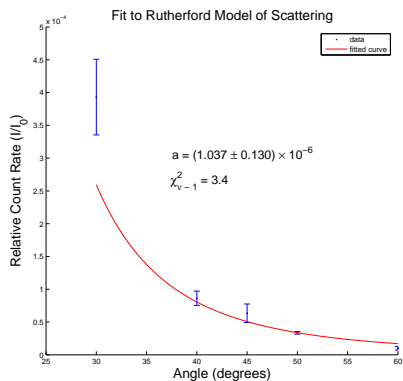


FIG. 4: Fit of convolved function with experimental data.

7. RESULTS

The values of $\frac{I}{I_0}$ were plotted against the angular position of the alpha particle source and then compared to the theoretical model (Figure 4). The theoretical fit model was obtained by convoluting the obtained beam profile with $(\frac{1}{\sin^4(\frac{\theta}{2})})$ and then fitting the constant in front of this convolved function to the experimentally obtained data, using a Matlab script. The obtained fit parameter was then compared with the constant in front of the Rutherford equation (Equation 2), $b = (\frac{ZZ'e^2}{4E})^2$. The theoretical value for the parameter b was calculated to be $1.76 \times 10^{-24} \text{cm}^2$.

To use our fit parameter a to calculate the experimental value of b , we used the following equation, which was obtained by using Equations 1 and 2:

$$b = \frac{a \times A_{Au}}{d\Omega \times \rho_{Au} \times x_{foil} \times N_{Av0}} = (7.81 \pm 5.35) \times 10^{-25} \text{cm}^2 \quad (4)$$

We find that the value obtained experimentally differs by an order of magnitude, although the large error brings it within range of the theoretical value. Reasons for this large error are discussed in the following section.

8. ERROR ANALYSIS

One source of random error in all components of this experiment was due the Poisson error, since the data was taken in the form of counts over a certain number of bins (in this case, channels in the MCS spectrum). This error propagated to the countrate, I .

In the beam attenuation measurements, the chief source of systematic error was the uncertainty in determining the energy peak of the alpha particle beam in the MCS spectrum.

The dominating systematic error in both the beam profile and gold foil scattering measurements was the uncer-

tainty in determining the angular position of the alpha particle source with respect to the normal of the detector surface—it was difficult to align the source precisely. In the final plots for both beam profile and gold scattering, this error in θ , or error in the x-coordinate, was converted into an error in the y-coordinate by using the slope of the expected function. In the case of the beam profile, the slope of the sides of the triangle were used, and in the case of the angular dependence scattering plot, the slope of the convoluted function of the beam profile with $(\frac{1}{\sin^4(\frac{\theta}{2})})$ was used. Once the x-coordinate error had been converted to a y-coordinate error, it was added in quadrature to the random error.

Another source of systematic error was in the determination of the beam profile, critical to determining what function with which to convolve the theoretical Rutherford scattering equation. Our beam profile function was necessarily rough, since it had a limited number of points.

One source of random error that was not accounted for was the noise that was caused by the detector in the lower channels of the MCS spectrum—the location of this noise varied from day to day and sometimes made it difficult to determine the true number of the total counts. This random error might explain the large deviation of the 20° measurement in the graph of the gold foil scattering data. The 20° still appears to be approximately within two standard deviations of the fit curve, however, and the reduced chi-squared of the fit has a reasonable value of 3.4.

9. CONCLUSIONS

The value obtained for the constant coefficient in front of the equation for the Rutherford differential scattering cross section was determined to be $(7.81 \pm 5.35) \times 10^{-25} \text{cm}^2$, compared to the theoretical value of $1.76 \times 10^{-24} \text{cm}^2$. The $\chi^2_{\nu-1}$ was found to be 3.4, which is on the order of 1 and is quite reasonable. Our experimental value was therefore within range of the theoretical value. It was concluded that the scattering behavior predicted by Rutherford was correct in describing the scattering of alpha particles off gold foil. The thickness of the foil was also determined to be $(9.256 \pm 0.711)10^{-3} \text{g/cm}^2$ and $(15.78 \pm 0.439)10^{-3} \text{g/cm}^2$ for four layers and eight layers of gold foil, respectively, using beam attenuation measurements. Improvements that could be made to this experiment would be to determine the energy and atomic number dependence of Rutherford scattering. Also, taking measurements at more angles, particularly at larger angles for longer integration times, would lead to a better experimental curve with which to compare against the theoretical model. One could also more finely define the curve of the beam profile, which would lead to a more accurate fit model for the gold scattering experimental data.

-
- [1] J. L. Staff, *Junior lab reader* (1990).
 - [2] A. Melissinos, *Experiments in Modern Physics: Interaction of Charged Particles with Matter* (Academic Press, 1966), chap. 5, pp. 152–165.
 - [3] A. Melissinos, *Experiments in Modern Physics: Rutherford Scattering* (Academic Press, 1966), chap. 6, pp. 226–252.
 - [4] A. Melissinos, *Experiments in Modern Physics: Solid State Detectors* (Academic Press, 1966), chap. 8.5, pp. 344–354.
 - [5] *Stopping power and range tables for helium ions*, URL <http://physics.nist.gov/PhysRefData/Star/Text/ASTAR.html>.

Acknowledgments

The author thanks David Greenspan for collaborating on this experiment, and also thanks Prof. Yamamoto, Sean Patrick, and Scott Sewell for assistance in the laboratory.